

November, 2025

Quantum Electron Clouds near Black Holes: Black Atoms and Molecules

Hinako Iseki^{1a}, Shin Sasaki^{1b}, and Kenta Shiozawa^{2c}

¹*Department of Physics, Kitasato University
Sagamihara 252-0373, JAPAN*

²*Center for Natural Sciences, College of Liberal Arts and Sciences,
Kitasato University
Sagamihara 252-0373, JAPAN*

Abstract

We study quantum mechanical wave functions near highly curved spaces, i.e., black holes. By utilizing the formalism developed by DeWitt, we derive the Schrödinger equations in the vicinity of the Schwarzschild and the Reissner–Nordström black hole geometries. The quantum electron cloud for the “black hydrogen atom”—an electron trapped by black holes—is particularly studied. We solve the equations and find that black holes generally attract the wave functions, localizing them near the horizon where the electrons are most likely to be trapped. These results imply that not only classical objects but also the quantum material and even the chemical properties of the atoms are affected by strong gravity. We also discuss black hydrogen molecules composed of multicentered Majumdar–Papapetrou black holes.

^aiseki.hinako(at)st.kitasato-u.ac.jp

^bshin-s(at)kitasato-u.ac.jp

^cshiozawa.kenta(at)kitasato-u.ac.jp

Contents

1	Introduction	1
2	Schrödinger equation in curved space	3
3	Quantum wavefunction near Schwarzschild black hole	5
3.1	Free particle near black hole	6
3.2	Attractive force by potential	8
4	Black hole atoms	11
4.1	Black hole hydrogen atom	11
4.2	Extremal limit	15
4.3	Overextremal case	16
5	Black hole molecule	17
6	Conclusion and discussions	20

1 Introduction

The quantization of gravity remains a difficult issue in modern physics. Despite many efforts, we have not reached any essential understanding of quantum theory of gravity. On the other hand, the relationship between quantum mechanical objects and gravity is also a subject that deserves investigation. Regarding this issue, relativistic quantum field theories in curved spacetimes have been developed [1].

Since gravity is the weakest fundamental interaction in nature, it is usually ignored in quantum theory of elementary particles. However, it is obvious that in strong gravitational systems, such as black holes, effects of gravity cannot be ignored. A typical example is the Hawking radiation of a black hole arising from the pair production/annihilation of particles in curved spacetimes [2, 3]. There are many studies on quantum natures of particles in black hole backgrounds, for example, see Refs. [4–8]. Very recently, quantum effects in curved spaces have been experimentally examined [9].

On the other hand, the fate of the quantum matters of intermediate scales such as $1\text{ \AA} = 10^{-10}\text{ m}$ near black holes has been the subject of relatively few investigations. There are several works along this line. These include one electron atom in general curved spacetimes [10, 11], effects of gravity on the hydrogen spectrum [12], a bound state of relativistic scalar particles and a rotating black hole [13], a nonrelativistic limit of scalar and Dirac fields in curved spacetimes [14, 15], gravitational effects by topological defects on the hydrogen atom [16], and general

relativistic effects on hydrogen systems [17]. There is no doubt that the quantum behavior of matters of atomic scale is best studied in the nonrelativistic quantum mechanics. Their quantum mechanical properties, including the detail of the material, the atomic, and the chemical properties, are completely understood by the solutions to the Schrödinger equation. It is now tantalizing to study how the strong gravity affects on the quantum wave functions in the atomic scale. It is apparent that effects of strong gravity near a black hole cannot be captured by simply introducing a Newtonian potential in the Schrödinger equation. The Newtonian approximation is valid when a quantum system is far from the black hole, namely, $r \gg r_H$, where r_H is the radius of the black hole event horizon. In order to examine the strong gravitational effects on quantum systems near the horizon at $r \sim r_H$, where the Newtonian approximation is violated, the Schrödinger equation that incorporates curvature effects of spacetime is required.

To this end, we utilize the formalism developed by DeWitt [18]. In this formalism, based on the general procedure of the analytical mechanics in the curved configuration space, the quantum mechanical Schrödinger equation in curved spaces is derived. Although this formalism subsequently developed into the quantization of gravity, including the Wheeler–DeWitt equation [19], we use it here to investigate the effects of gravity on quantum matters of atomic scale. We note that this nonrelativistic treatment is guaranteed by the local Lorentz description of the slowly moving condition. We assume that the local energy and the velocity for particles of mass m obey $E_{\text{loc}} \ll mc^2$ and $v_{\text{loc}} \ll c$. We also assume that the tidal condition $|R^{\mu}_{\nu\rho\sigma}| \lambda^2 \ll 1$ is fulfilled in the parameter ranges we consider, so that the de Broglie wavelength λ is much shorter than the curvature radius. This means that the energy scale of quantum particles is smaller than that of the gravitational tidal forces. The condition allows us to utilize the nonrelativistic approximation. Throughout this paper, we focus on black holes of atomic scale. Then the tidal force condition remains true except within an extremely close region of the horizon where $|R^{\mu}_{\nu\rho\sigma}|^{-\frac{1}{2}}$ and λ are of the same order of magnitude, i.e., the Bohr radius of the hydrogen. Therefore, we are interested in the region $r_H < r < \alpha r_H$, where α is an $\mathcal{O}(10^0 \sim 10^1)$ parameter. Quantum matters in the vicinity of black holes in other formalisms have been studied, such as quantum mechanics of constrained particles [20], quantum mechanical particles near black holes using Fermi coordinates [21–23], and so on.

The organization of this paper is as follows. In the next section, we briefly introduce the Schrödinger equation in curved spaces that is developed by DeWitt [18]. In Sec. 3, we write down the Schrödinger equation in the Schwarzschild black hole background. We explicitly show the equations in the spherical coordinate that result from the canonical quantization based on the Cartesian coordinate. We decompose the equation by the variable separation and then study the radial equation by introducing a virtual electric potential. We show that the Schrödinger equation reduces to the confluent Heun’s differential equation, ensuring that it is solved analytically. We then solve the equation with an appropriate boundary condition and

show that the quantum electron cloud is mostly trapped just on the event horizon. We visualize the wave functions and find that the probability densities are strongly affected by the black hole. In Sec. 4, we discuss the charged black holes. We study the quantum wave functions in the backgrounds of the nonextremal, extremal, and overextremal Reissner–Nordström black holes. The wave functions in the regions inside the inner (Cauchy) and outside the outer (event) horizons are studied. We find that the famous gravitational repulsion force near the core of the Reissner–Nordström black hole is observed in the wave function. The extremal limit and the overextremal cases are also discussed. In Sec. 5, we discuss the black hole molecule that consists of the two extremal black hole nuclei and one electron. This corresponds to the hydrogen molecular ion H_2^+ . We show that in a specific region of parameters, the equations can be solved analytically. Sec. 6 is devoted to the conclusion and discussions. We discuss a possible realization of the black hole atoms in the present Universe.

2 Schrödinger equation in curved space

In this section, we briefly introduce the formalism developed by DeWitt [18]. A nonrelativistic particle with mass μ moving in a curved configuration space is governed by the following Lagrangian:

$$L = \frac{\mu}{2} g_{ij} \dot{q}^i \dot{q}^j + a_i \dot{q}^i - V(q), \quad (2.1)$$

where g_{ij} is a spatial metric of the configuration space spanned by the coordinates q^i , and $V(q)$ is a potential. Here, $\dot{q}^i = \frac{dq^i}{dt}$, and t is a parameter that specifies the particle motion. The vector potential a_i should be included when we consider background magnetic fields. The Riemann and the Ricci curvature tensors associated with the spatial metric g_{ij} are defined as

$$\begin{aligned} R^{(3)i}_{jkl} &= \partial_k \Gamma^i_{jl} - \partial_l \Gamma^i_{jk} + \Gamma^i_{pk} \Gamma^p_{jl} - \Gamma^i_{pl} \Gamma^p_{jk}, \\ \Gamma^i_{jk} &= \frac{1}{2} g^{ip} \left(\partial_j g_{kp} + \partial_k g_{jp} - \partial_p g_{jk} \right), \\ R^{(3)}_{ij} &= R^{(3)k}_{ikj}, \\ R^{(3)} &= g^{ij} R^{(3)}_{ij}, \end{aligned} \quad (2.2)$$

where g^{ij} is the inverse of g_{ij} .

The canonical quantization condition is defined by

$$[q^i, q^j] = 0, \quad [q^i, p_j] = i\hbar \delta^i_j, \quad [p_i, p_j] = 0, \quad (2.3)$$

where p_i is the canonical momentum conjugate to q^i . The quantum Hamiltonian \hat{H}_\pm receives

the curvature and the metric corrections¹,

$$\begin{aligned}\hat{H}_\pm &= \hat{H} \pm \frac{\hbar^2}{12} R^{(3)}, \\ \hat{H} &= \frac{1}{2\mu} g^{-\frac{1}{4}} (p_i - a_i) g^{\frac{1}{2}} g^{ij} (p_j - a_j) g^{-\frac{1}{4}} + V,\end{aligned}\quad (2.4)$$

where $g = \det g_{ij}$. The coordinate representation for the canonical momentum p_i is given by

$$p_i = -i\hbar \left(\frac{\partial}{\partial q^i} + \frac{1}{4} \frac{\partial}{\partial q^i} \log g \right). \quad (2.5)$$

In order to ensure the conservation of the probability, the t -derivative of the wave function ψ is modified in the curved space,

$$\frac{\partial \psi}{\partial t} \rightarrow \frac{D\psi}{Dt} = \frac{\partial \psi}{\partial t} + \frac{1}{4} \left(\frac{\partial}{\partial t} \log g \right) \psi. \quad (2.6)$$

In the end, the Schrödinger equation in the curved space is obtained as

$$i\hbar \frac{D\psi}{Dt} = \hat{H}_+ \psi. \quad (2.7)$$

Here, the Hamiltonian \hat{H}_+ is given in (2.4). For later convenience, we rewrite the equation in the explicit form. In the following, we consider $a_i = 0$ and q^i as the Cartesian coordinate x^i ($i = 1, 2, 3$) for a three-dimensional space. Then, the momentum is given by

$$\hat{p}_i = -i\hbar \left(\hat{A}_i + \frac{1}{4} B_i \right), \quad \hat{A}_i = \frac{\partial}{\partial x^i}, \quad B_i = \frac{1}{g} \frac{\partial g}{\partial x^i}. \quad (2.8)$$

The curvature-independent part of the Hamiltonian \hat{H} in (2.4) is evaluated as

$$\begin{aligned}\hat{H} &= \frac{1}{2\mu} g^{-\frac{1}{4}} \hat{p}_i g^{\frac{1}{2}} g^{ij} \hat{p}_j g^{-\frac{1}{4}} + V \\ &= -\frac{\hbar^2}{2\mu} g^{-\frac{1}{4}} \left[\hat{A}_i g^{\frac{1}{2}} g^{ij} \hat{A}_j g^{-\frac{1}{4}} + \frac{1}{4} B_i g^{\frac{1}{2}} g^{ij} \hat{A}_j g^{-\frac{1}{4}} + \frac{1}{4} \hat{A}_i g^{\frac{1}{2}} g^{ij} B_j g^{-\frac{1}{4}} + \frac{1}{16} B_i g^{\frac{1}{2}} g^{ij} B_j g^{-\frac{1}{4}} \right] + V.\end{aligned}\quad (2.9)$$

Note that the derivative \hat{A}_i acts on all parts of its right side including the wave function. By distributing the \hat{A}_i to the relevant terms and collecting the terms altogether, we have the explicit form of the Schrödinger equation,

$$i\hbar \left(\frac{\partial \psi}{\partial t} + \frac{1}{4g} \frac{\partial g}{\partial t} \psi \right) = -\frac{\hbar^2}{2\mu} \left\{ \frac{1}{2} g^{ij} \frac{1}{g} \frac{\partial g}{\partial x^i} \frac{\partial \psi}{\partial x^j} + \frac{\partial g^{ij}}{\partial x^i} \frac{\partial \psi}{\partial x^j} + g^{ij} \left(\frac{\partial}{\partial x^i} \frac{\partial}{\partial x^j} \psi \right) \right\} + \left\{ V(x) + \frac{\hbar^2}{12} R^{(3)} \right\} \psi. \quad (2.10)$$

¹Note that there is a potential ambiguity on the quantum Hamiltonian. We have two equivalent choices $\hat{H}_\pm = \hat{H} \pm \frac{\hbar^2}{12} R^{(3)}$ that are consistent with the classical limit $\hbar \rightarrow 0$. We here employ \hat{H}_+ rather than \hat{H}_- for definiteness. This kind of nonuniqueness of quantum theory in curved space is often recognized. See [24], for example.

It is easy to show that the flat space limit $g_{ij} = \delta_{ij}$ results in the ordinary Schrödinger equation.

In the following, we focus on the stationary state for ψ and assume that the background metric g_{ij} is independent of t . In this case, we have $\frac{\partial g}{\partial t} = 0$, and the wave function is decomposed as $\psi(t, x) = e^{-i\frac{E}{\hbar}t}\psi(x)$, where E is a constant. Then, the equation for $\psi(x)$ is found to be

$$-\frac{\hbar^2}{2\mu} \left\{ \frac{1}{2} g^{ij} \frac{1}{g} \frac{\partial g}{\partial x^i} \frac{\partial}{\partial x^j} + \frac{\partial g^{ij}}{\partial x^i} \frac{\partial}{\partial x^j} + g^{ij} \left(\frac{\partial}{\partial x^i} \frac{\partial}{\partial x^j} \right) \right\} \psi(x) + \left\{ V(x) + \frac{\hbar^2}{12} R^{(3)} \right\} \psi(x) = E\psi(x). \quad (2.11)$$

3 Quantum wavefunction near Schwarzschild black hole

In this section, we consider the four-dimensional Schwarzschild black hole as the prototypical example of curved space. The Schwarzschild solution in the Cartesian coordinate is given by

$$ds^2 = - \left(1 - \frac{a}{r} \right) (dx^0)^2 + \sum_{k=1}^3 (dx^k)^2 + \frac{a}{r^2(r-a)} \left(\sum_{k=1}^3 x^k dx^k \right)^2, \quad (3.1)$$

where $r^2 = x^2 + y^2 + z^2$, and $a = \frac{2G_N M}{c^2}$ is a constant. A three-dimensional spatial geometry arises from the time slice of the metric (3.1). The point $r = a$ corresponds to the event horizon that the spatial metric diverges. The spatial metric in the Cartesian coordinate in the matrix notation is given by

$$g_{ij} = \begin{pmatrix} 1 + \frac{ax^2}{r^2(r-a)} & \frac{axy}{r^2(r-a)} & \frac{axz}{r^2(r-a)} \\ \frac{ayx}{r^2(r-a)} & 1 + \frac{ay^2}{r^2(r-a)} & \frac{ayz}{r^2(r-a)} \\ \frac{azx}{r^2(r-a)} & \frac{azy}{r^2(r-a)} & 1 + \frac{az^2}{r^2(r-a)} \end{pmatrix}, \quad g^{ij} = \begin{pmatrix} 1 - \frac{ax^2}{r^3} & -\frac{axy}{r^3} & -\frac{axz}{r^3} \\ -\frac{axy}{r^3} & 1 - \frac{ay^2}{r^3} & -\frac{ayz}{r^3} \\ -\frac{azx}{r^3} & -\frac{ayz}{r^3} & 1 - \frac{az^2}{r^3} \end{pmatrix}. \quad (3.2)$$

Then we have $g = \det g_{ij} = \frac{r}{r-a}$ and $R^{(3)} = 0$. We stress that we should begin with the Cartesian coordinate rather than the radial one since the canonical quantization condition (2.3) is justified only in the former coordinate system. We obtain the correct quantum mechanical equation in the spherical coordinate (r, θ, ϕ) by starting from (3.1) in the (x, y, z) system and then switch to the (r, θ, ϕ) system at the final stage of the calculations.

After tedious calculations, we find that Eq. (2.11) in the (r, θ, ϕ) coordinate is given by

$$-\frac{\hbar^2}{2\mu} \left\{ \left(1 - \frac{a}{r} \right) \frac{\partial^2}{\partial r^2} + \left(\frac{2}{r} - \frac{3a}{2r^2} \right) \frac{\partial}{\partial r} + \frac{1}{r^2} \frac{\partial^2}{\partial \theta^2} + \frac{1}{r^2 \sin^2 \theta} \frac{\partial^2}{\partial \phi^2} + \frac{\cos \theta}{r^2 \sin \theta} \frac{\partial}{\partial \theta} \right\} \psi + V\psi = E\psi. \quad (3.3)$$

The wave function is decomposed as $\psi(r, \theta, \phi) = R(r)Y_l^m(\theta, \phi)$. Then, we find that the equations for each part are given by

$$\begin{aligned} \left(1 - \frac{a}{r}\right) \frac{\partial^2 R}{\partial r^2} + \left(\frac{2}{r} - \frac{3a}{2r^2}\right) \frac{\partial R}{\partial r} + \left\{ \frac{2\mu}{\hbar^2} (E - V) - \frac{l(l+1)}{r^2} \right\} R = 0, \\ \frac{1}{\sin^2 \theta} \frac{\partial^2 Y_l^m}{\partial \phi^2} + \frac{1}{\sin \theta} \frac{\partial}{\partial \theta} \left(\sin \theta \frac{\partial Y_l^m}{\partial \theta} \right) + l(l+1)Y_l^m = 0, \end{aligned} \quad (3.4)$$

where $l = 0, 1, 2, \dots$ are constants. The equation for Y_l^m is the same as the one in the flat space. Then, $Y_l^m(\theta, \phi)$ is found to be the spherical harmonics

$$\begin{aligned} Y_l^m(\theta, \phi) = \sqrt{\frac{2l+1}{4\pi} \frac{(l-m)!}{(l+m)!}} P_l^{|m|}(\cos \theta) e^{im\phi} \\ (l = 0, 1, 2, \dots, m = -l, -l+1, \dots, l-1, l), \end{aligned} \quad (3.5)$$

where $P_l^{|m|}(x)$ is the Legendre polynomial.

We next study the equation for the radial direction. Depending on whether the particles are in a bound state or not, we must set the boundary conditions appropriately.

3.1 Free particle near black hole

Before discussing bound states, we first consider the case of the free particle $V = 0$. The equation for the radial direction is given by

$$\left(1 - \frac{a}{r}\right) \frac{d^2 R}{dr^2} + \left(\frac{2}{r} - \frac{3a}{2r^2}\right) \frac{dR}{dr} + \left(k^2 - \frac{l(l+1)}{r^2}\right) R = 0, \quad (3.6)$$

where we have assumed $E > 0$ and defined $k^2 = \frac{2\mu E}{\hbar^2}$. We can show that Eq. (3.6) has regular singular points at $r = 0$ and $r = a$. The indicial equation of (3.6) reveals that the solutions at $r = a$ behave like $R(r) \sim (r - a)^0$ and $(r - a)^{\frac{1}{2}}$. Then, $R(r)$ is regular but $R'(r)$ for $R(r) \sim (r - a)^{\frac{1}{2}}$ diverges at the horizon. Since the radial coordinate r in (3.1) becomes timelike in $r < a$ and thus it ceases to be a suitable coordinate for the wave function, we look for smooth solutions outside the horizon $r > a$. The Schwarzschild solution is asymptotically flat, and solutions to Eq. (3.6) must approach the ones in the flat space. It is easy to show that in the asymptotic flat regime $r \rightarrow \infty$, the equation has the solution given by the spherical Bessel functions that behave as $R(r) \sim \frac{1}{r} e^{\pm ikr}$.

For consistency, we examine the equation in the asymptotic limit $r \gg a$. In this region, the equation is compared to that in the flat space. After rearranging the coefficient of R'' to be unity and by the rescaling² $\hat{R} = (1 + \frac{a}{4r}) R$, the equation results in the form

$$\hat{R}''(r) + \frac{2}{r} \hat{R}'(r) + \left(k^2 - \frac{l(l+1)}{r^2} + \frac{ak^2}{r}\right) \hat{R}(r) = 0, \quad (3.7)$$

²This rescaling arises from matching the integral measure to that of the flat space $\sqrt{g}|R|^2 \rightarrow |R|^2$. Namely, $R \rightarrow g^{-\frac{1}{4}}R = (1 - \frac{a}{r})^{-\frac{1}{4}}R \sim (1 + \frac{a}{4r})R$.

where we have ignored $\mathcal{O}(r^{-3})$ terms. This is the equation in the flat space with the effective Newtonian potential $V \propto -\frac{1}{r}$. Therefore, particles sufficiently away from the black hole certainly perceive the Newtonian gravity.

We now rewrite Eq. (3.6). By introducing the dimensionless coordinate $x = \frac{r}{a}$ and substituting $R(x) = e^{\sigma x} H(x)$, Eq. (3.6) becomes the following form:

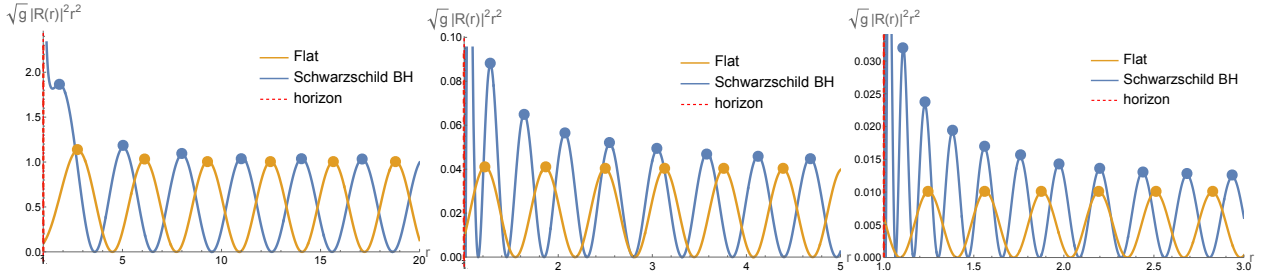
$$H''(x) + \left\{ \frac{\frac{3}{2}}{x} + \frac{\frac{1}{2}}{x-1} + 2\sigma \right\} H'(x) + \frac{1}{x(x-1)} \left\{ (2\sigma + a^2 k^2)x - \frac{3}{2}\sigma - l(l+1) \right\} H(x) = 0, \quad (3.8)$$

where we have set $\sigma = \pm i a k$. We find that (3.8) is the confluent form of Heun's differential equation. The parameters³ are $\gamma = \frac{3}{2}$, $\delta = \frac{1}{2}$, $\varepsilon = 2\sigma = \pm 2i a k$, $\alpha = 2\sigma + a^2 k^2$, and $q = -\frac{3}{2}\sigma - l(l+1)$. The general solution is, therefore, given by $R(r) = e^{\pm i k r} H(r)$, where $H(r)$ is the confluent Heun function defined by the parameters given above. The signs \pm correspond to the outgoing and ingoing modes, respectively. The confluent Heun function has two linearly independent asymptotic expansions at $x \rightarrow \infty$: $H(x) \sim x^{-\alpha/\varepsilon}$ and $H(x) \sim e^{-\varepsilon x} x^{-\gamma-\delta+\alpha/\varepsilon}$ [25]. The physically relevant solution that behaves as $R(r) \sim \frac{1}{r} e^{\pm i k r}$ ($r \rightarrow \infty$) corresponds to the first branch. Physically, this implies that a purely outgoing or ingoing mode at infinity originates from the scattering of waves at the horizon. The local analysis at $r = a$ gives $R \sim A + B\sqrt{r-a}$, where A, B are constants. A boundary condition at infinity, which we will take such that $R \sim \frac{\sin kr}{r}$ is a real-valued function, fixes a particular linear combination of these two local behaviors through the global properties of the confluent Heun function, or equivalently, through a numerical integration.

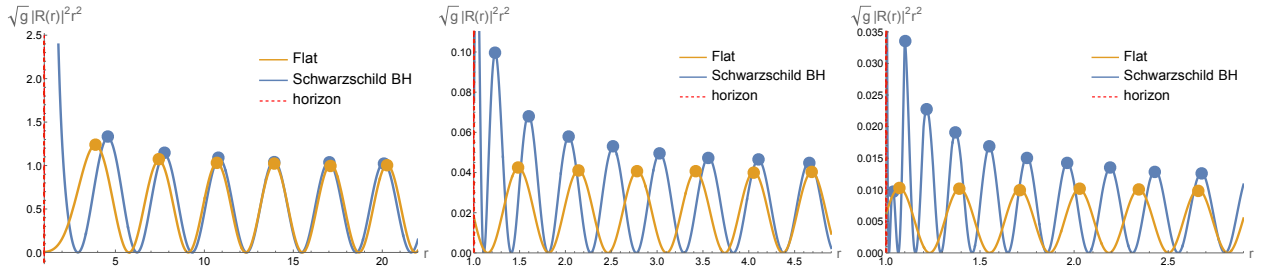
In order to see the behavior of the wave function near the black hole, it is useful to visualize the solution. To this end, we solve the equation numerically and make plots. The probability density $\sqrt{g}|R(r)|^2 r^2$ in the radial direction is shown in Fig. 1.

We find that the wave function is most strongly attracted near the horizon. At the same time, the wave function exhibits overall shifts toward the black hole direction. Note that although $R(r)$ itself is finite at $r = a$, the probability density diverges at the horizon due to the factor $\sqrt{g} = \sqrt{\frac{r}{r-a}}$. It is also observed that the higher the energy, the more it is attracted toward the center. This can be confirmed by comparing the distance between any two peaks in the wave function. As the energy increases by $k = 1, 5, 10$, the distances between any adjacent peaks become smaller. A naive interpretation of this fact is that objects with higher energy (mass) are attracted more strongly by gravity. These characteristic behaviors indicate that quantum particles are also strongly affected by gravity. The 3D plots in Fig. 2 clearly show how gravity affects the wave function. Note that we employ real-valued solutions for $R(r)$. This

³The standard form of Heun's differential equation of confluent type is $H''(z) + \left[\frac{\gamma}{z} + \frac{\delta}{z-1} + \varepsilon \right] H'(z) + \frac{\alpha z - q}{z(z-1)} H(z) = 0$.



(a) Radial probability density of the $l = 1$.



(b) Radial probability density of the $l = 2$.

Figure 1: The probability density $\sqrt{g}|R(r)|^2r^2$ in the radial direction. Comparison between the flat space and the black hole background cases for $a = 1$. (a) $l = 1$ with $k = 1$ (left), $k = 5$ (middle), and $k = 10$ (right), and (b) $l = 2$ with $k = 1$ (left), $k = 5$ (middle), and $k = 10$ (right). The red dotted line corresponds to the event horizon $r = a$. The infinity is set to be $r_{\max} = 1000$ and we define the boundary condition $R(r_{\max}) = 0$ to find the numerical solutions with *Mathematica*. The normalization factors are appropriately chosen.

means that the linear combination of the ingoing and outgoing modes produces the standing wave, resulting in the vanishing of the radial current of probability $j_r \propto R\partial_r\bar{R} - \bar{R}\partial_rR = 0$.

In the following, we introduce an electric attractive force potential and examine a bound state in the black hole background.

3.2 Attractive force by potential

In the next section, we will discuss a genuine ‘‘black hole hydrogen atom,’’ namely, a negatively charged particle trapped by a positively charged black hole. Before discussing this truly ideal situation, we first consider a simpler setup, i.e., a particle subject to a hypothetical attractive potential in the Schwarzschild geometry. We stress that the Schwarzschild black hole cannot support a static electric potential in the strict sense. A charged source would inevitably change the Schwarzschild geometry to the one for the Reissner–Nordström solution. However, before proceeding to the rigorous treatment of the case in the next section, we first examine this setting as a simplified toy model to find the effects of the curved background on the hydrogenlike

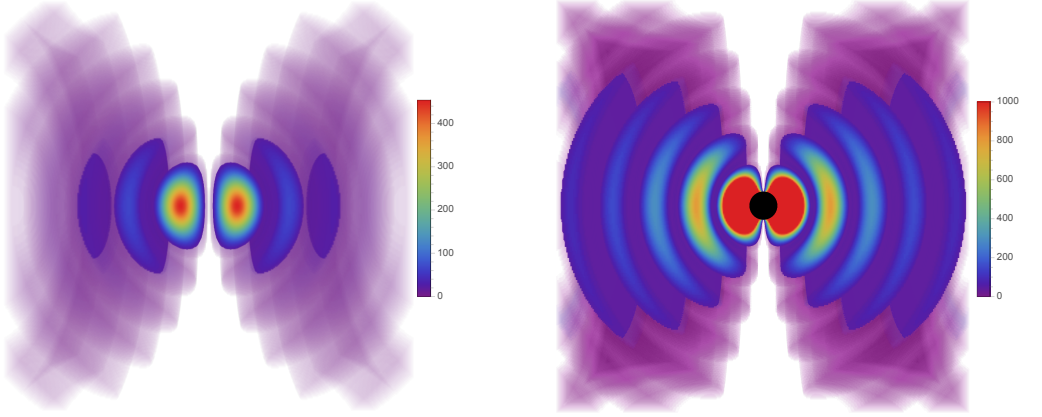


Figure 2: The 3D plots for the probability density $|\psi(r, \theta, \phi)|^2$ for free particles. The cases of flat space (left) and the black hole background (right). The parameters are fixed to $a = 1$, $l = 1$, and $k = 1$. The values increase from blue to red and the event horizon is shown in the black sphere.

potential. This setup is justified by introducing a small probe charge to the Schwarzschild black hole and ignoring its backreaction to the geometry. We assume that there is the potential $V = -\frac{e^2}{r}$ producing an electriclike attractive force. We here employ the unit $4\pi\varepsilon_0 = 1$, and e is the charge of the particle. We call this electron in the following. The equation in the radial direction is given by

$$\left(1 - \frac{a}{r}\right) \frac{d^2R}{dr^2} + \left(\frac{2}{r} - \frac{3a}{2r^2}\right) \frac{dR}{dr} + \left\{ \frac{2\mu}{\hbar^2} \left(E + \frac{e^2}{r}\right) - \frac{l(l+1)}{r^2} \right\} R = 0. \quad (3.9)$$

We find that $r = 0$ and $r = a$ are the regular singular points. At the horizon $r = a$, the solution behaves like $R(r) \sim (r - a)^0$ and $(r - a)^{\frac{1}{2}}$. Then, $R(r)$ is regular but $R'(r)$ for the latter case diverges at $r = a$.

Since the geometry is asymptotically flat, the equation coincide with the ordinary one for the hydrogen atom in $r \rightarrow \infty$. In this regime the solution should coincides with the well-known wave function. Since the energy spectrum of the hydrogen atom is determined by the asymptotic boundary condition, we can employ the energy spectrum $E_n = -\frac{\mu e^4}{2n^2 \hbar^2}$ ($n = 1, 2, 3, \dots$) for the flat space even in the presence of the black hole. Following the prescription presented in the previous subsection, we find that the equation for the radial direction $R(x) = e^{i\sigma x} H(x)$ is given by

$$H''(x) + \left\{ 2\sigma + \frac{\frac{3}{2}}{x} + \frac{\frac{1}{2}}{x-1} \right\} H'(x) + \frac{1}{x(x-1)} \left\{ (2\sigma - a^2 \kappa^2 + as^2)x - \frac{3}{2}\sigma - l(l+1) \right\} H(x) = 0, \quad (3.10)$$

where we have again defined $x = \frac{r}{a}$, $\sigma = \pm a\kappa$, $\kappa^2 = \frac{-2\mu E_n}{\hbar^2}$, and $s^2 = \frac{2\mu e^2}{\hbar^2}$. The general solution

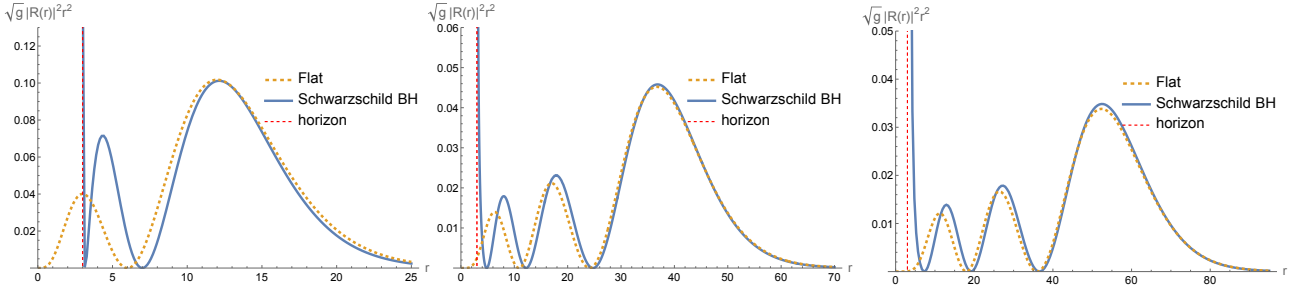


Figure 3: The radial probability densities of the wave function $\sqrt{g}|R(r)|^2r^2$. Comparison between the hydrogen atom in the flat space and in the black hole background cases for $a = 1$. The figures correspond to the $3p$ orbital ($n = 3, l = 1$) (left), the $5d$ orbital ($n = 5, l = 2$) (middle), and the $6f$ orbital ($n = 6, l = 3$) (right) of the hydrogen atom. We will always use the parameters $\mu = e = \hbar = 1$ in the following.

is, therefore, given by the confluent Heun's function $H(\gamma, \delta, \varepsilon, \alpha, q, x)$, where the parameters are given by $\gamma = \frac{3}{2}$, $\delta = \frac{1}{2}$, $\varepsilon = 2\sigma$, $\alpha = 2\sigma - a^2\kappa^2 + as^2$, and $q = -\frac{3}{2}\sigma - l(l+1)$.

We find that it is convenient to visualize the wave function by solving the equation numerically. To this end, we rewrite Eq. (3.9) into the following form:

$$(\rho - 2\kappa a) \frac{\partial^2 u}{\partial \rho^2} + \left\{ 2(l+1 + \kappa a) - \rho - \frac{\kappa a}{\rho}(4l+3) \right\} \frac{\partial u}{\partial \rho} + \left\{ n - l - 1 - \frac{\kappa a}{2} - \frac{\kappa a l}{\rho^2}(2l+1) + \frac{\kappa a}{\rho} \left(\frac{3}{2} + 2l \right) \right\} u = 0, \quad (3.11)$$

where we have defined $\rho = 2\kappa r$ and $R(\rho) = \rho^l e^{-\frac{\rho}{2}} u(\rho)$. We employ the boundary condition $R \rightarrow 0$ ($r \rightarrow \infty$). Then the solutions are shown in Figs. 3 and 4. Even though the wave function is strongly concentrated near the horizon, the peak appears to be displaced to outside when it is slightly farther away from the horizon. This behavior can be interpreted as follows. Although electrons are gravitationally attracted toward the black hole and extremely localized in a thin shell near the horizon, the uncertainty principle causes their kinetic energy to increase when they are too close to the horizon surface. Interestingly, the localization of electrons due to the strong gravitational attraction of the black hole has the opposite effect of repulsing particles away from it. These two forces balance to minimize the energy, resulting in a finite spread and peak positions of the wave function. Paradoxically, the stronger the gravitational attraction toward the center, the farther the electrons are pushed away. The difference between the bound state and the free particle discussed in Sec. 3.1 is that the former makes standing waves and localizes sharply, while the latter does not. Then it is natural that the former is more subject to the uncertainty relation.

However, when the black hole becomes sufficiently large, the situation changes. Figure 5 shows a comparison of the radial probability densities obtained by varying the horizon position

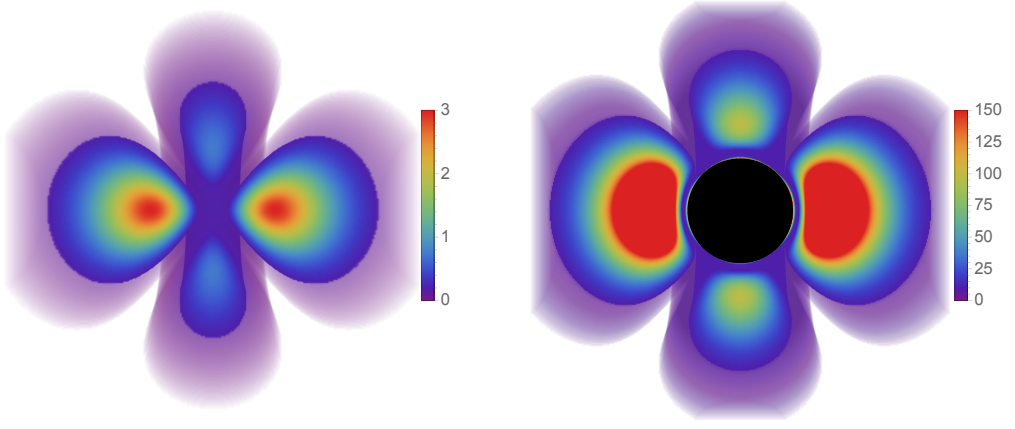


Figure 4: The 3D plot of the probability density $|\psi|^2$ for the particle under the attractive force. The flat space (left) and the black hole background (right) cases. The figures correspond to the $3d$ orbital ($n = 3, l = 2$) of the hydrogen atom. The values increase from blue to red and the event horizon $a = 5$ is shown in the black color.

$$r = a.$$

When the horizon position changes, the peak positions of the wave function move accordingly. By changing the horizon position and making it larger than the peak position of the probability density, the corresponding peak appears to be absorbed into the horizon. Then gravity eventually prevails over the quantum effects and electrons will inevitably localize on the horizon.

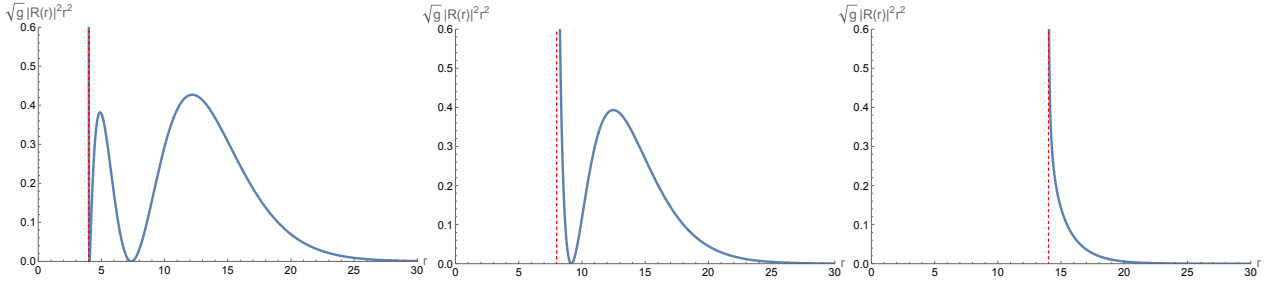
4 Black hole atoms

We now study the genuine ‘‘black hole atoms.’’ We introduce the single nonextremal Reissner–Nordström black hole as the positively charged atomic nucleus. In the following, we examine the quantum wave function for a negatively charged particle trapped by the black hole. This is nothing but the hydrogen atom composed of a black hole nucleus and an electron.

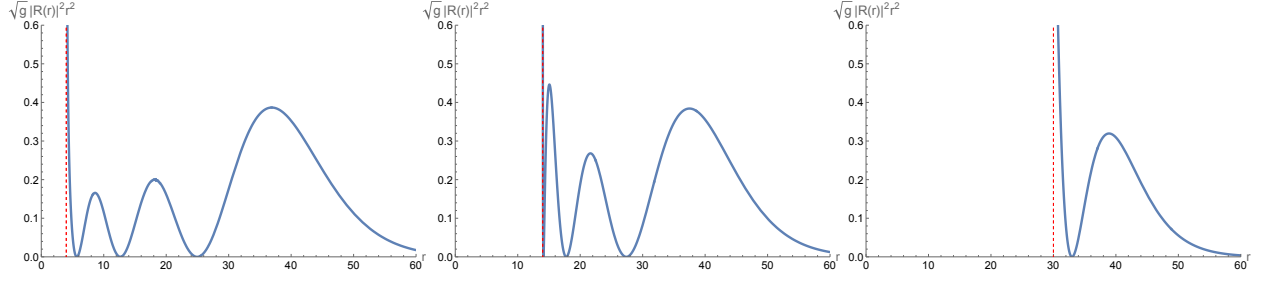
4.1 Black hole hydrogen atom

The nonextremal Reissner–Nordström black hole metric in the Cartesian coordinate is given by

$$ds^2 = - \left(1 - \frac{a}{r} + \frac{Q^2}{r^2} \right) (dx^0)^2 + \sum_{k=1}^3 (dx^k)^2 + \frac{ra - Q^2}{r^2(r^2 - ra + Q^2)} \left(\sum_{k=1}^3 x^k dx^k \right)^2, \quad (4.1)$$



(a) Radial probability density of the 3p orbital.



(b) Radial probability density of the 5d orbital.

Figure 5: Comparison of the radial probability density $\sqrt{g} |R(r)|^2 r^2$ of (a) the 3p orbital ($n = 3, l = 1$) and (b) the 5d orbital ($n = 5, l = 2$) for different a values in the Schwarzschild background with the potential V . Each figure shows $a = 4$ (left), $a = 8$ (middle), and $a = 14$ (right) for the 3p orbital, and $a = 4$ (left), $a = 14$ (middle), and $a = 30$ (right) for the 5d orbital. The red dotted line denotes the event horizon.

where $r^2 = x^2 + y^2 + z^2$, and $a = \frac{2G_{NM}}{c^2}$ and $Q^2 = \frac{G_N e^2}{c^4}$ are constants. The outer and the inner horizons are at $r = r_+$ and $r = r_-$, respectively, where we have defined $r_{\pm} = \frac{a \pm \sqrt{a^2 - 4Q^2}}{2}$. The gauge field $A_0 = -\frac{1}{c} \frac{e}{r}$ in the solution provides the electrostatic potential. The time slice of the solution (4.1) gives a three-dimensional spatial curved space. The spatial metric is given by

$$g_{ij} = \begin{pmatrix} 1 + x^2 f & xyf & xzf \\ xyf & 1 + y^2 f & yzf \\ xzf & yzf & 1 + z^2 f \end{pmatrix},$$

$$g^{ij} = \frac{1}{1 + r^2 f} \begin{pmatrix} 1 + (y^2 + z^2)f & -xyf & -xzf \\ -xyf & 1 + (x^2 + z^2)f & -yzf \\ -xzf & -yzf & 1 + (x^2 + y^2)f \end{pmatrix},$$

$$f = \frac{ra - Q^2}{r^2(r^2 - ra + Q^2)}. \quad (4.2)$$

The Ricci scalar of the three-dimensional space is calculated as

$$R^{(3)} = \frac{2Q^2}{r^4}. \quad (4.3)$$

We also have $g = \det g_{ij} = \frac{r^2}{(r-r_+)(r-r_-)}$. Then, after some calculations, the Schrödinger equation in the (r, θ, ϕ) system is given by

$$\begin{aligned} & -\frac{\hbar^2}{2\mu} \left\{ \left(1 - \frac{ar - Q^2}{r^2}\right) \frac{\partial^2}{\partial r^2} + \left(\frac{2}{r} - \frac{3ar - 2Q^2}{2r^3}\right) \frac{\partial}{\partial r} + \frac{1}{r^2} \frac{\partial^2}{\partial \theta^2} + \frac{\cos \theta}{r^2 \sin \theta} \frac{\partial}{\partial \theta} + \frac{1}{r^2 \sin^2 \theta} \frac{\partial^2}{\partial \phi^2} \right\} \psi \\ & + \frac{\hbar^2 Q^2}{6r^4} \psi - \frac{e^2}{r} \psi = E\psi. \end{aligned} \quad (4.4)$$

Note that the Coulomb potential $V = -\frac{e^2}{r}$ that gives the electromagnetic attractive force is naturally incorporated through the coupling $eCA_0\psi$ in the Schrödinger equation. This differs from the case of the Schwarzschild black hole where we have introduced a hypothetical potential by hand.

By substituting the decomposition $\psi(r, \theta, \phi) = R(r)Y(\theta, \phi)$ in the equation, we find that the angular function $Y(\theta, \phi)$ satisfies the same equation in the Schwarzschild case, and hence it is the spherical harmonics. On the other hand, the equation in the radial direction is given by

$$\left(1 - \frac{ar - Q^2}{r^2}\right) \frac{\partial^2 R}{\partial r^2} + \left(\frac{2}{r} - \frac{3ar - 2Q^2}{2r^3}\right) \frac{\partial R}{\partial r} + \left\{ \frac{Q^2}{3r^4} + \frac{2\mu}{\hbar^2} \left(E + \frac{e^2}{r}\right) - \frac{l(l+1)}{r^2} \right\} R = 0. \quad (4.5)$$

It is shown that $r = 0$ and $r = r_{\pm}$ are regular singular points. At $r \sim 0$, the solution behaves like

$$R(r) \underset{r \rightarrow 0}{\sim} \exp \left[i \sqrt{\frac{1}{3Q}} \ln r \right], \quad R'(r) \underset{r \rightarrow 0}{\sim} \frac{1}{r} \exp \left[i \sqrt{\frac{1}{3Q}} \ln r \right]. \quad (4.6)$$

Therefore, $R(r)$ is regular but $R'(r)$ diverges at $r = 0$. Near the horizons $r \sim r_{\pm}$, the solution behaves like

$$R(r) \underset{r \rightarrow r_{\pm}}{\sim} (r - r_{\pm})^0, \quad (r - r_{\pm})^{\frac{1}{2}}. \quad (4.7)$$

Then, $R(r)$ is regular at the horizons, but for $R(r) \sim (r - r_{\pm})^{\frac{1}{2}}$ its derivative diverges, as in the case of the Schwarzschild black hole. Now we look for bound states where $E < 0$. The asymptotic consistency again results in $E_n = -\frac{\mu e^4}{2n^2 \hbar^2}$. Using the same parameters as discussed before, Eq. (4.5) is rewritten as

$$\begin{aligned} & (\rho^2 - 2\kappa a \rho + 4\kappa^2 Q^2) \frac{\partial^2 u}{\partial \rho^2} + \left\{ -\rho^2 + 2\rho(l+1+\kappa a) - \kappa a(4l+3) + \frac{4\kappa^2 Q^2}{\rho} (2l+1-\rho) \right\} \frac{\partial u}{\partial \rho} \\ & + \left[\rho \left(n - l - 1 - \frac{\kappa a}{2} \right) + \kappa a \left(2l + \frac{3}{2} \right) - \left\{ \frac{\kappa a l}{\rho} + \frac{2\kappa^2 Q^2}{\rho} \right\} (2l+1) + \frac{4\kappa^2 Q^2}{\rho^2} \left(l^2 + \frac{1}{3} \right) + \kappa^2 Q^2 \right] u = 0, \end{aligned} \quad (4.8)$$

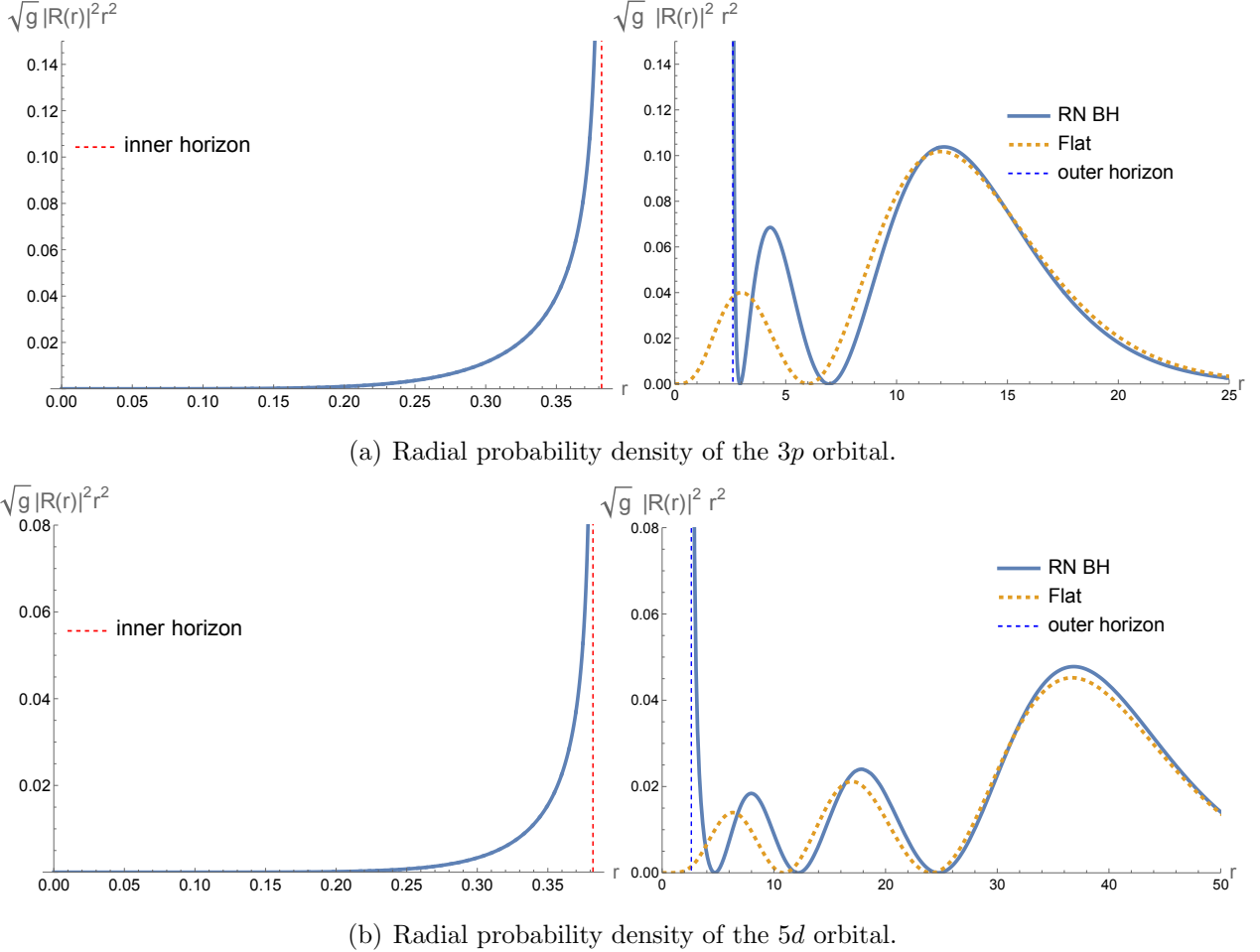


Figure 6: The probability density $\sqrt{g}|R(r)|^2r^2$ in the radial direction. Comparison between the flat space and the Reissner–Nordström black hole (RN BH) background for $a = 3$ and $Q = 1$. Inside the inner horizon (left) and outside the outer horizon (right). The figure corresponds to (a) the 3p orbital ($n = 3, l = 1$) and (b) the 5d orbital ($n = 5, l = 2$) of the hydrogen atom.

where $\rho = 2\kappa r$ and $R(r) = \rho^l e^{-\frac{\rho}{2}} u(\rho)$ as in the case of Eq. (3.11). We solve this equation numerically. The numerical visualization of the wave functions is shown in Fig. 6.

The region outside the outer horizon behaves similarly to the case of the Schwarzschild black hole. The wave function is strongly attracted to the outer horizon. On the other hand, we find that within the region inside the inner horizon, the wave function is attached to the inner horizon from the interior. This behavior is most naturally interpreted as the effect of the gravitational repulsion force observed near the core of the Reissner–Nordström black hole [26, 27]. This repulsive force is intuitively understood from the fact that $g_{00} \sim -\frac{a}{r} + \frac{Q^2}{r^2}$ in (4.1) can be identified with the gravitational potential in the weak gravity approximation. In the region $r \gg a$, the attractive force from $-\frac{a}{r}$ is dominant, while in the small r region, the repulsive force from $\frac{Q^2}{r^2}$ overcomes the former.

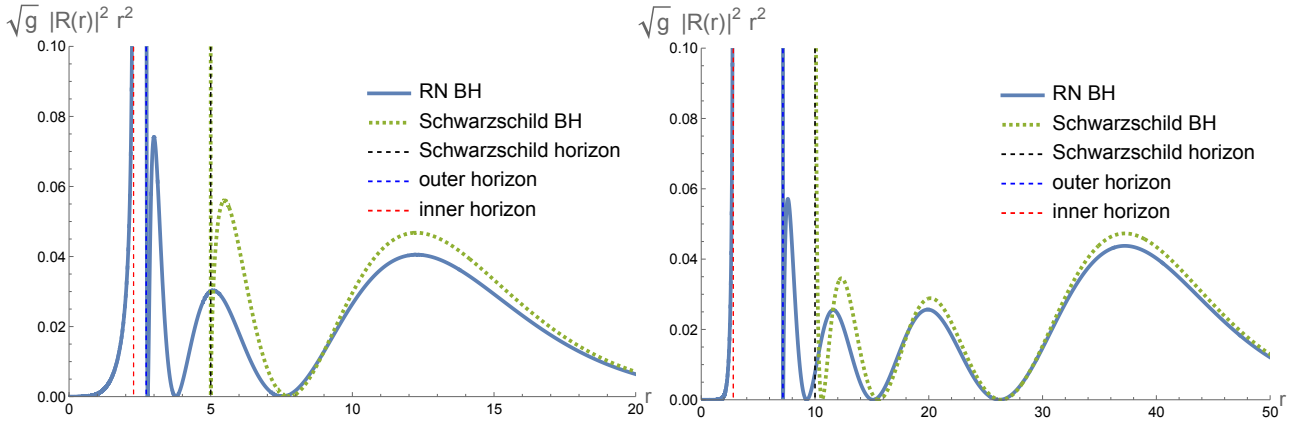


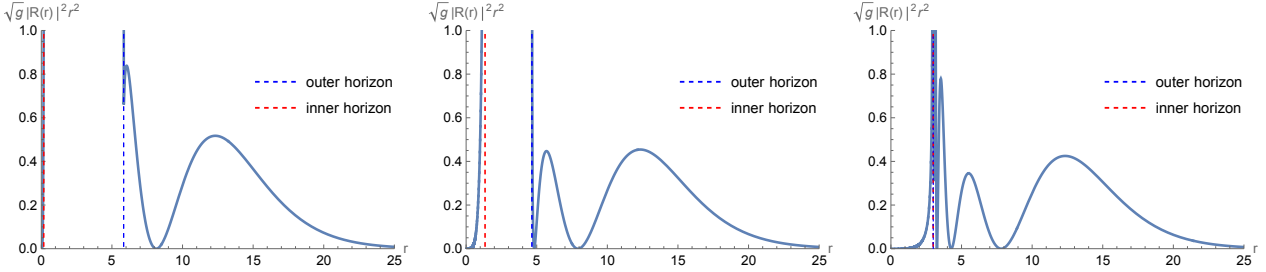
Figure 7: Comparison of the radial probability density in the Schwarzschild black hole and the Reissner–Nordström black hole backgrounds. The left figure shows the $3p$ orbital ($n = 3, l = 1$) with the parameters fixed at $a = 5$ and $Q = 2.49$, while the right figure shows the $5d$ orbital ($n = 5, l = 2$) with the parameters fixed at $a = 10$ and $Q = 4.5$. In the Reissner–Nordström case, new peaks appear near the outer horizon, indicating the characteristic influence of the electromagnetic charge on the radial distribution. There appear new peaks close to the outer horizon in the Reissner–Nordström case.

The radial probability densities for the Schwarzschild and the Reissner–Nordström black holes are shown in Fig. 7. We observe that there appear new peaks in the Reissner–Nordström black hole background which are absent in the flat and the Schwarzschild cases. We can see that the radial wave function $R(r)$ oscillates more rapidly when it closes to $r = r_+$. This indicates that there appear more stable orbits of electrons in the vicinity of horizons and we expect that the chemical property of the black hydrogen atom is quite different from the ordinary one.

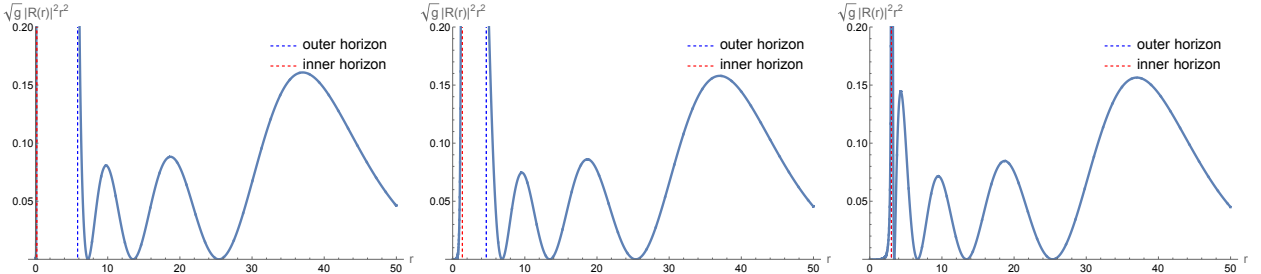
4.2 Extremal limit

In the extremal limit $a^2 = 4Q^2$, the two horizons coincide, $r_+ = r_-$. The behavior of the solution (4.7) is inherited to this case. As we approach the extremum $4Q^2 \rightarrow a^2$, the distance between the inner and the outer horizons decreases and it becomes eventually zero at $4Q^2 = a^2$. In this limit, the gravitational repulsion takes place just inside the degenerate horizon.

Figure 8 shows the radial probability density. Here, the ratio of the charges between the black hole and the electron is fixed. As Q^2 increases, the position of the outer horizon moves inward. As the horizon shifts toward the center, the peaks of the wave function that were previously “eaten away” reappear. This is because increasing Q with fixed a results in a smaller horizon. We can refer to the previous discussion in the Schwarzschild background. At the same time, as the black hole approaches the extremum, the wave function approaches the horizon from both inside and outside and it forms a shell of the high probability density at



(a) Radial probability density of the 3p orbital.



(b) Radial probability density of the 5d orbital.

Figure 8: The radial probability density $\sqrt{g}|R(r)|^2r^2$ of (a) the 3p orbital ($n = 3, l = 1$) and (b) the 5d orbital ($n = 5, l = 2$) in the Reissner–Nordström case. We fix $a = 6$ and vary Q toward the extremal limit $Q = 3$. Each figure shows $Q = 1$ (left), $Q = 2.5$ (middle), and $Q = 3$ (right).

the degenerated horizon. This is an electron configuration unique to the black hole atom, not typically observed in the ordinary hydrogen atom. The 3D plots of the probability density $|\psi|^2$ are shown in Fig. 9.

4.3 Overextremal case

Finally, we examine the overextremal case $4Q^2 > a^2$. In this case, there are no horizons and it appears naked singularity at $r = 0$. Even though there is the naked singularity, the solution $R(r)$ is regular at $r = 0$. Now the repulsive term $\frac{Q^2}{r^2}$ strongly dominates over the attractive one $-\frac{a}{r}$ in the overextremal case $Q^2 \gg a^2$ in the effective potential $V \sim -\frac{a}{r} + \frac{Q^2}{r^2}$. This, therefore, should push the wave function further outward from the naked singularity. The radial probability density in the overextremal case is shown in Fig. 10. We find the expected behavior of the wave functions. Interestingly, we find that a new peak appears near the naked singularity. This may be explained by the gravitational repulsion and the quantum effect. Namely, particles pushed outward by the strong repulsion are pushed back toward the center by the exclusion principle. This corresponds to the inverse of the phenomenon where the particles localized at the center by gravitational attraction are pushed outward by the exclusion principle.

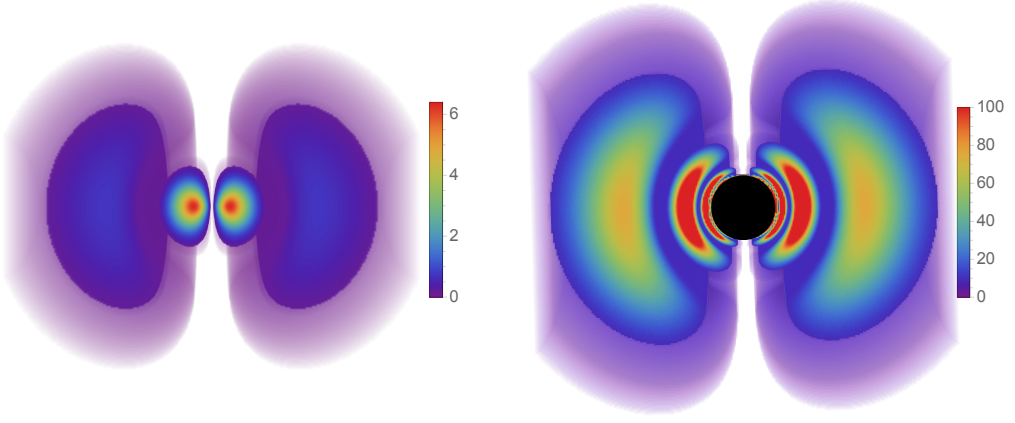


Figure 9: The 3D plots of the probability density $|\psi|^2$ for the hydrogen atom in the $3p$ orbital. The flat (left) and the extremal black hole backgrounds (right). The parameters are fixed to $a = 6$ and $Q = 3$. The values increase from blue to red and the event horizon is shown in the black color.

5 Black hole molecule

According to elementary chemistry, when two atomic nuclei share electrons, a hydrogen molecule is formed. In particular, the hydrogen molecular ion H_2^+ , where two atomic nuclei share a single electron, is known as a model that can be solved exactly. It is now natural to examine the “black hole molecule” that consists of two black hole hydrogen atoms. This is composed of the two stable charged black holes together with the quantum electrons that are trapped by them. We consider the multicentered Majumdar–Papapetrou black hole solution as the nuclei of the molecule. The Majumdar–Papapetrou solution in four dimensions is given by

$$ds^2 = -U^{-2}(dx^0)^2 + U^2(dx^2 + dy^2 + dz^2), \quad A = U^{-1}dx^0, \quad (5.1)$$

where U is the harmonic function in \mathbb{R}^3 ,

$$U = 1 + \sum_{i=1}^N \frac{M_i}{R_i}, \quad R_i^2 = (x - x_i)^2 + (y - y_i)^2 + (z - z_i)^2. \quad (5.2)$$

Here, M_i ($i = 1, \dots, N$) are constants and (x_i, y_i, z_i) are centers of the black holes in \mathbb{R}^3 . Each black hole in the Majumdar–Papapetrou solution (5.1) is stable since the gravitational attraction and the electromagnetic repulsion are balanced.

We now focus on the $N = 2$ binary black holes as the prototypical example. In this case, the three-dimensional Ricci scalar is calculated as

$$R^{(3)} = \frac{2 \left\{ M_2^2 R_1^4 + M_1^2 R_2^4 + 2M_1 M_2 R_1 R_2 (\vec{R}_1 \cdot \vec{R}_2) \right\}}{\left(M_2 R_1 + M_1 R_2 + R_1 R_2 \right)^4}, \quad (5.3)$$

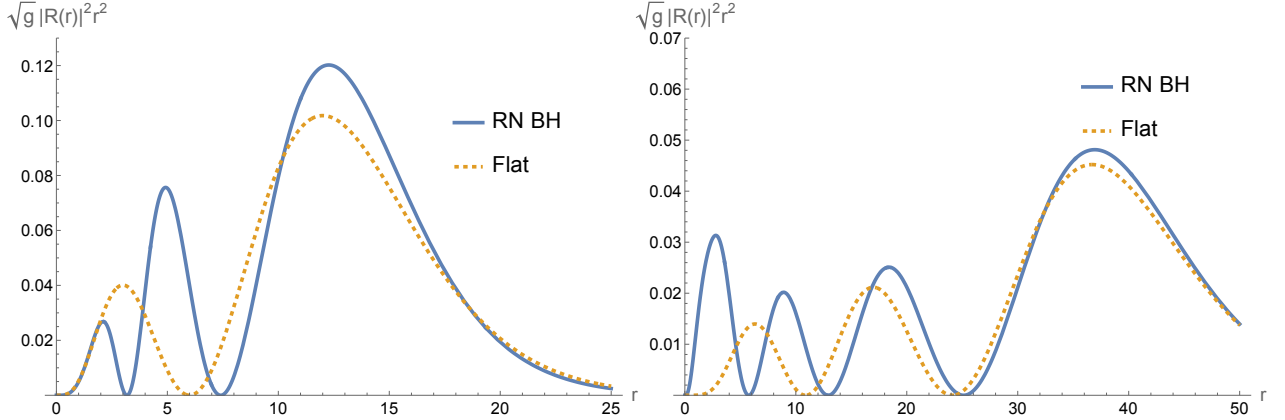


Figure 10: Comparison of the numerical solution of the radial probability density $\sqrt{g}|R(r)|^2r^2$ in the overextremal Reissner–Nordström background and in the flat space. The parameters are fixed to $a = 5$ and $Q = 3$. The point $r = 0$ represents the naked singularity. The figure on the left corresponds to the $3p$ orbital ($n = 3, l = 1$) of the hydrogen atom and that on the right to the $5d$ orbital ($n = 5, l = 2$).

where $\vec{R}_i = (x - x_i, y - y_i, z - z_i)$ ($i = 1, 2$). As in the case of the ordinary hydrogen molecule in the flat space, we employ the Born–Oppenheimer approximation. Namely, we ignore the dynamics of the nuclei (the binary black holes). We also consider a single electron trapped on them for simplicity. This corresponds to the hydrogen molecular ion H_2^+ composed of the black holes having each charge $+e$ and a single electron with mass μ and the charge $-e$. Then the Schrödinger equation is given by

$$\begin{aligned} -\frac{\hbar^2}{2\mu} \left\{ \frac{1}{U^2} \nabla^2 \psi + \frac{1}{U^3} (\nabla U \cdot \nabla \psi) \right\} - \left(\frac{e^2}{R_1} + \frac{e^2}{R_2} \right) \psi \\ + \frac{\hbar^2}{12} \frac{2 \left\{ M_2^2 R_1^4 + M_1^2 R_2^4 + 2M_1 M_2 R_1 R_2 (\vec{R}_1 \cdot \vec{R}_2) \right\}}{(M_2 R_1 + M_1 R_2 + R_1 R_2)^4} = E\psi. \end{aligned} \quad (5.4)$$

where we have included the potential $V(r) = -\frac{e^2}{R_1} - \frac{e^2}{R_2}$ that provides the electromagnetic attractive force.⁴ For the standard H_2^+ case, a variable separation is possible by using the spheroidal coordinates. We assume that the two black holes are located on the points $(0, 0, -d/2)$ and $(0, 0, d/2)$ in \mathbb{R}^3 and $M_1 = M_2 = M$ (Fig. 11).

It is convenient to employ the coordinates

$$\xi = \frac{R_1 + R_2}{d}, \quad \eta = \frac{R_1 - R_2}{d}. \quad (5.5)$$

⁴For the ordinary hydrogen molecular ion H_2^+ , the potential includes $V(r) = \frac{e^2}{R_{12}}$ that represents the repulsive force between two nuclei. It is obvious that in our setup, such repulsive force does not exist.

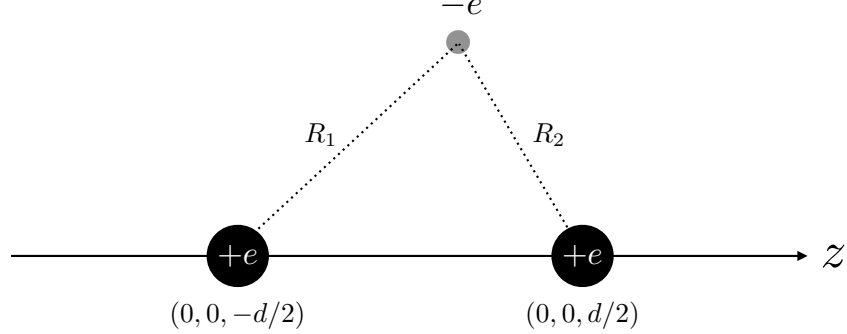


Figure 11: A schematic picture of the hydrogen molecular ion H_2^+ composed of two charged black holes and an electron.

These together with an azimuth angle ϕ consist of the spheroidal coordinates. They are defined in $1 \leq \xi < \infty$, $-1 \leq \eta \leq 1$, and $0 \leq \phi < 2\pi$. These are related to the Cartesian coordinate as

$$x = \frac{d}{2} \sqrt{(\xi^2 - 1)(1 - \eta^2)} \cos \phi, \quad y = \frac{d}{2} \sqrt{(\xi^2 - 1)(1 - \eta^2)} \sin \phi, \quad z = \frac{d}{2} \xi \eta. \quad (5.6)$$

By using this coordinate system, the Laplacian becomes

$$\nabla^2 = \frac{4}{d^2(\xi^2 - \eta^2)} \left[\frac{\partial}{\partial \xi} \left((\xi^2 - 1) \frac{\partial}{\partial \xi} \right) + \frac{\partial}{\partial \eta} \left((1 - \eta^2) \frac{\partial}{\partial \eta} \right) + \left(\frac{1}{\xi^2 - 1} + \frac{1}{1 - \eta^2} \right) \frac{\partial^2}{\partial \phi^2} \right]. \quad (5.7)$$

We also have

$$R^{(3)} = -\frac{128M^2(\xi^2 - \eta^2 - 3\eta^2\xi^2 - \xi^4)}{\{4M\xi - d(\xi^2 - \eta^2)\}^4}, \quad U = 1 + \frac{4M}{d} \frac{\xi}{\xi^2 - \eta^2}. \quad (5.8)$$

Then, using the decomposition $\psi(\xi, \eta, \phi) = R(\xi)S(\eta)e^{i\alpha\phi}$, the Schrödinger equation (5.4) becomes

$$\begin{aligned} & \frac{1}{R} \frac{d}{d\xi} \left\{ (\xi^2 - 1) \frac{d}{d\xi} R \right\} + \frac{1}{S} \frac{d}{d\eta} \left\{ (1 - \eta^2) \frac{d}{d\eta} S \right\} - \frac{\alpha^2}{\xi^2 - 1} - \frac{\alpha^2}{1 - \eta^2} \\ & - \frac{1}{4} \frac{4M(\xi^2 + \eta^2)(\xi^2 - 1)}{(\xi^2 - \eta^2) \{d(\xi^2 - \eta^2) + 4M\xi\}} \frac{1}{R} \frac{dR}{d\xi} - \frac{1}{4} \frac{8M\eta\xi(1 - \eta^2)}{(\xi^2 - \eta^2) \{d(\xi^2 - \eta^2) + 4M\xi\}} \frac{1}{S} \frac{dS}{d\eta} \\ & + \left(1 + \frac{4M}{d} \frac{\xi}{\xi^2 - \eta^2} \right)^2 \left(dA\xi + \frac{2\mu d^2}{3} (\xi^2 - \eta^2) \frac{128M^2(\xi^2 - \eta^2 - 3\eta^2\xi^2 - \xi^4)}{\{4M\xi - d(\xi^2 - \eta^2)\}^4} - \kappa^2 d^2 (\xi^2 - \eta^2) \right) = 0, \end{aligned} \quad (5.9)$$

where we have defined $A = \frac{2\mu e^2}{\hbar^2}$, $\kappa^2 = -\frac{2\mu E}{\hbar^2}$, and used the following relation:

$$\vec{\nabla}U \cdot \vec{\nabla}\psi = \frac{1}{d^2} \left[\frac{\xi^2 - 1}{\xi^2 - \eta^2} \frac{\partial U}{\partial \xi} \frac{\partial}{\partial \xi} \psi + \frac{1 - \eta^2}{\xi^2 - \eta^2} \frac{\partial U}{\partial \eta} \frac{\partial}{\partial \eta} \psi + \frac{1}{(\xi^2 - 1)(1 - \eta^2)} \frac{\partial U}{\partial \phi} \frac{\partial}{\partial \phi} \psi \right]. \quad (5.10)$$

We find that the ϕ dependence is decoupled but the ξ and η sectors are not. This is expected since the Stäckel condition of the equation is violated by the curvature corrections. Therefore, the equation is solved by the numerical analysis.

In order to solve the equation analytically, it is necessary to decouple the two variables ξ and η . To this end, we consider a specific limit $\mu \rightarrow 0$ with fixed M . This corresponds to the limit where the mass of the electron is small compared to the mass of the black hole, and is a natural assumption. Then the third line in (5.9) is ignored, and the terms in the second line in the large- ξ region become $-\frac{M}{d} \frac{1}{R} \frac{dR}{d\xi}$. Then the equation in this asymptotic region becomes

$$\begin{aligned} \frac{d}{d\xi} \left\{ (\xi^2 - 1) \frac{d}{d\xi} R \right\} - \frac{M}{d} \frac{dR}{d\xi} - \left(\Lambda + \frac{\alpha^2}{\xi^2 - 1} \right) R &= 0, \\ \frac{d}{d\eta} \left\{ (1 - \eta^2) \frac{d}{d\eta} S \right\} + \left(\Lambda - \frac{\alpha^2}{1 - \eta^2} \right) S &= 0, \end{aligned} \quad (5.11)$$

where Λ is a parameter. Now in this specific regime and parameters, the two equations are decoupled and can be solved analytically. Note that the effects of the black holes $M \neq 0$ still remain in these equations. We find solutions given by

$$\begin{aligned} R(\xi) &= \left(\frac{1 - \xi}{1 + \xi} \right)^{\frac{M}{2d}} \left(c_1 P_A^B(\xi) + c_2 Q_A^B(\xi) \right), \\ S(\eta) &= c_3 P_A^\alpha(\eta) + c_4 Q_A^\alpha(\eta), \end{aligned} \quad (5.12)$$

where $P_A^B(x)$ and $Q_A^B(x)$ are the associated Legendre functions of the first and the second kinds, respectively. The parameters are given by $A = \frac{1}{2}(\sqrt{4\Lambda + 1} - 1)$ and $B = \frac{1}{2d}\sqrt{M^2 + 4d^2\alpha^2}$, and c_1, \dots, c_4 are integration constants. The single-valuedness of the wave function requires that α be an integer. If we require the discrete energy spectra and the normalizability for bound states, A and B would be integers satisfying the conditions $0 \leq B \leq A$ and $0 \leq \alpha \leq A$. It is known that the exact solution for the ordinary hydrogen molecule ion H_2^+ is given by the associated Legendre polynomials $P_n^m(x)$ and the confluent Heun function $H(x)$ [28]. Although the solution (5.12) has a similar structure with the ordinary H_2^+ in the sense that they share the Legendre polynomials, they are of course different due to the curvature corrections and the absence of the internuclei potential.

6 Conclusion and discussions

In this paper, we studied quantum wave functions near black holes. To this end, we utilized the formalism developed by DeWitt [18]. The equation itself has been known for a long time, but to our knowledge, this is the first time that it is applied to black holes and its solutions are analyzed. We in particular focused on the hydrogen atom type configuration, namely, a

single electron trapped by black holes. We considered time slices of the Schwarzschild and Reissner–Nordström black hole geometries and explicitly wrote down equations.

We first derived the equation for free particle in the spatial geometry of the Schwarzschild black hole. We found that the equation is rewritten in the form of the confluent Heun equation and it is, therefore, solved analytically. In order to visualize the wave function, we found it convenient to solve the equation numerically. We showed that the wave function is attracted toward the black hole and observed that particles with higher energy are more strongly attracted. We then introduced a hypothetical electric attractive potential to the Schwarzschild black hole and studied the bound states. The equation is again rewritten in the form of the confluent Heun equation. We numerically found solutions satisfying appropriate boundary conditions and visualized the wave functions for the hydrogen atom type configuration. We found that the wave function and the electron cloud are attracted into the horizon and are confined around the horizon.

Next, we focused on the charged black hole and discussed the genuine black hole atom. We considered the Reissner–Nordström black hole solution and derived the Schrödinger equation. Assuming a spherically symmetric solution, we numerically solved the equation in the radial direction. We then examined the effects of the black hole on the hydrogen atom for various quantum numbers. We visualized the wave function, explicitly showing the difference from the ordinary hydrogen atom. We observed that the electron cloud is generically bound to the outer horizon. We also investigated the wave function extending into the region inside the inner horizon. We observed that the wave function is attracted to the inner horizon from the interior. This is most naturally interpreted as the famous gravitational repulsion force present in the $r \sim 0$ region of the Reissner–Nordström black hole. These results indicate that not only classical objects but also quantum wave functions are affected by gravity. This is obvious intuitively (classically), but not evident in quantum theory. We also studied the wave functions in the extremal and the overextremal cases.

We then derived the Schrödinger equation for a molecule with a binary black hole as its nucleus. It is known that the Schrödinger equation for the hydrogen molecular ion H_2^+ in flat spacetime can be solved exactly. We consider Majumdar–Papapetrou black holes as the nucleus. Since there is no force acting between these black holes, it is in some sense simpler than ordinary molecules. However, due to the presence of the curvature term, the spheroidal coordinates variables cannot be separated. Therefore, numerical analysis is generally required. We demonstrated that under specific conditions, the equation becomes separable and analytical solutions can be obtained.

It would be helpful to know whether the black hole discussed in this paper is available in the current Universe or not. The Schwarzschild radius of a black hole of mass M is given by $r_0 = \frac{2G_N M}{c^2}$, where G_N is Newton’s gravitational constant. On the other hand, the Bohr

radius of the hydrogen atom is known as $a_0 = \frac{4\pi\varepsilon_0\hbar^2}{m_e e^2} \sim 10^{-10} \text{ m}$ (where m_e is the mass of the electron). The mass of the black holes of the size of the hydrogen atom is estimated as $M = \frac{c^2 a_0}{2G_N} \sim 6.7 \times 10^{16} \text{ kg}$, which is of the same order as the small asteroid. Black holes of such a small mass are not created by the gravitational collapse of stars but may appear in the early stage of the Universe. The time Δt that it takes for a black hole of mass $M \sim 10^{16} \text{ kg}$ to disappear through the Hawking radiation is estimated as $\Delta t \sim \frac{G_N}{\hbar c^3} M^3 \sim 10^{24} \text{ yr}$, which is greater than the age of the Universe. Therefore, it is possible that it remains in the current Universe as a primordial black hole. It cannot be excluded that such black holes trap electrons and form the “atoms” discussed in this paper.

An interesting consideration related to what we discussed here is the discrepancy between the classical and quantum depictions of black hole atoms. In the purely classical picture, a test electron that is not supported by any nongravitational force and has insufficient angular momentum cannot remain at rest near a black hole. In such a situation, the electron cannot help crossing the horizon in a finite proper time along its timelike geodesic. In contrast, in the ordinary hydrogen atom in the flat space, quantum mechanics prevents the electron from collapsing into the nucleus and instead provides stationary bound states. Our results suggest an analogous mechanism for the “black hole atom,” namely, quantum effects can support bound states of the electron even in regions where classical motion admits no stable circular orbit so that the electron does not necessarily fall into the black hole. The “gravity versus quantum” effects is an interesting issue to study. It would be interesting to study this issue in more complex black holes, such as Kerr solutions and so on.

Acknowledgments

The work of S. S. and K. S. is supported by Grant-in-Aid for Scientific Research, JSPS KAKENHI Grant Number JP25K07324. The work of K. S. is also supported by the Kitasato University Research Grant for Young Researchers.

References

- [1] R. M. Wald, *Quantum Field Theory in Curved Space-Time and Black Hole Thermodynamics*, University of Chicago Press, 1995. ISBN 978-0-226-87027-4.
- [2] S. W. Hawking, “Black Hole Explosions,” *Nature* **248** (1974), 30–31.
- [3] S. W. Hawking, “Particle Creation by Black Holes,” *Commun. Math. Phys.* **43** (1975), 199–220 [erratum: *Commun. Math. Phys.* **46** (1976), 206].

- [4] D. G. Boulware, “Quantum Field Theory in Schwarzschild and Rindler Spaces,” *Phys. Rev. D* **11** (1975), 1404.
- [5] J. B. Hartle and S. W. Hawking, “Path Integral Derivation of Black Hole Radiance,” *Phys. Rev. D* **13** (1976), 2188–2203.
- [6] W. G. Unruh, “Notes on Black Hole Evaporation,” *Phys. Rev. D* **14** (1976), 870.
- [7] D. N. Page, “Particle Emission Rates from a Black Hole: Massless Particles from an Uncharged, Nonrotating Hole,” *Phys. Rev. D* **13** (1976), 198–206.
- [8] M. K. Parikh and F. Wilczek, “Hawking Radiation as Tunneling,” *Phys. Rev. Lett.* **85** (2000), 5042–5045 [arXiv:hep-th/9907001 [hep-th]].
- [9] J. P. Covey, I. Pikovski, and J. Borregaard, “Probing Curved Spacetime with a Distributed Atomic Processor Clock,” *PRX Quantum* **6** (2025) no.3, 030310 [arXiv:2502.12954 [quant-ph]].
- [10] L. Parker, “One-Electron Atom in Curved Space-Time,” *Phys. Rev. Lett.* **44** (1980) no.23, 1559.
- [11] L. Parker, “One Electron Atom as a Probe of Space-Time Curvature,” *Phys. Rev. D* **22** (1980), 1922–1934.
- [12] L. Parker and L. O. Pimentel, “Gravitational Perturbation of the Hydrogen Spectrum,” *Phys. Rev. D* **25** (1982), 3180–3190.
- [13] S. Hod, “Quasi-Bound States of Massive Scalar Fields in the Kerr Black-Hole Spacetime: Beyond the Hydrogenic Approximation,” *Phys. Lett. B* **749** (2015), 167–171 [arXiv:1510.05649 [gr-qc]].
- [14] R. Falcone and C. Conti, “Nonrelativistic Limit of Scalar and Dirac Fields in Curved Spacetime,” *Phys. Rev. D* **107** (2023) no.4, 045012 [arXiv:2210.02405 [hep-th]].
- [15] U. D. Jentschura and J. H. Noble, “Nonrelativistic Limit of the Dirac-Schwarzschild Hamiltonian: Gravitational Zitterbewegung and Gravitational Spin-Orbit Coupling,” *Phys. Rev. A* **88** (2013), 022121 [arXiv:1306.0479 [gr-qc]].
- [16] G. de A. Marques and V. B. Bezerra, “Hydrogen Atom in the Gravitational Fields of Topological Defects,” *Phys. Rev. D* **66** (2002), 105011 [arXiv:gr-qc/0209030 [gr-qc]].
- [17] E. Fischbach, B. S. Freeman, and W. K. Cheng, “General Relativistic Effects in Hydrogenic Systems,” *Phys. Rev. D* **23** (1981), 2157 [erratum: *Phys. Rev. D* **24** (1981), 1702].

- [18] B. S. DeWitt, “Dynamical Theory in Curved Spaces. I. A Review of the Classical and Quantum Action Principles,” *Rev. Mod. Phys.* **29** (1957), 377–397.
- [19] B. S. DeWitt, “Quantum Theory of Gravity. I. The Canonical Theory,” *Phys. Rev.* **160** (1967), 1113–1148.
- [20] L. C. B. da Silva, C. C. Bastos, and F. G. Ribeiro, “Quantum Mechanics of a Constrained Particle and the Problem of Prescribed Geometry-induced Potential,” *Annals Phys.* **379** (2017), 13–33 [arXiv:1602.00528 [quant-ph]].
- [21] Q. Exirifard and E. Karimi, “Schrödinger Equation in a General Curved Spacetime Geometry,” *Int. J. Mod. Phys. D* **31** (2022) no.03, 2250018 [arXiv:2105.13896 [gr-qc]].
- [22] R. G. G. Amorim, V. Rispoli, S. Ulhoa, and K. V. S. Araújo, “Nonrelativistic Spinless Particle in Vicinity of Schwarzschild-like Black Hole,” *Int. J. Mod. Phys. A* **39** (2024) no.01, 2450005 [arXiv:2310.14241 [gr-qc]].
- [23] Q. Exirifard and E. Karimi, “Trajectory of a Massive Localized Wave Function in a Curved Spacetime Geometry,” *Phys. Rev. D* **107** (2023) no.6, 064059 [arXiv:2207.13182 [gr-qc]].
- [24] S. A. Fulling, “Nonuniqueness of Canonical Field Quantization in Riemannian Space-Time,” *Phys. Rev. D* **7** (1973), 2850–2862.
- [25] A. Ronveaux, *Heun’s Differential Equations*, Oxford University Press, 1995.
- [26] A. Qadir, “Reissner-Nordstrom Repulsion,” *Phys. Lett. A* **99** (1983), 419–420.
- [27] S. M. Mahajan, A. Qadir, and P. M. Valanju, “Reintroducing the Concept of «Force» into Relativity Theory,” *Nuovo Cimento* **65** (1981), 404–418.
- [28] D. R. Bates, K. Ledsham, and A. L. Stewart, “Wave Functions of the Hydrogen Molecular Ion,” *Phil. Trans. R. Soc. A* **246** (1953) no.911, 215–240.